Astrophys Space Sci (2016) 361:320
DOI 10.1007/s10509-016-2910-1

ORIGINAL ARTICLE

Study of the period changes in SW Dor, an RR Lyrae type star with Blazhko effect

L.N. Berdnikov[1,2] · A.Y. Kniazev[2,3,4] · A.K. Dambis[2] · V.V. Kravtsov[2,5] · R. Sefako[3]

Received: 20 April 2016 / Accepted: 17 August 2016

Abstract In 2012–2014 we acquired 1569 CCD BVI_c frames for the RR Lyrae type variable SW Dor with the 76-cm telescope of the South African Astronomical Observatory (SAAO) and 1-m telescopes of Las Cumbres Observatory Global Telescope network (LCOGT). Our observations showed a large scatter in the resulting phased light curve, especially near maximum brightness, which allowed us to reveal the Blazhko effect with a period of $\sim 80\overset{\mathrm{d}}{.}9$. To study the pulsation period changes, we used all the available observations including the 1299 magnitude estimates from the digitized plate library of Harvard University (the DASCH project), which allowed us to construct the $O-C$ diagram spanning a 125-year long time interval and discover for the first time at least three abrupt changes of the pulsation period.

Keywords Stars: variables: RR Lyrae · Stars: oscillations · Techniques: photometric · Galaxies: spirals

✉ A.K. Dambis
dambis@yandex.ru

L.N. Berdnikov
lberdnikov@yandex.ru

1 Astronomy and Astrophysics Research division, Entoto Observatory and Research Center, P.O. Box 8412, Addis Ababa, Ethiopia

2 Sternberg Astronomical Institute, Lomonosov Moscow State University, Universitetskii pr. 13, Moscow, 119992, Russia

3 South African Astronomical Observatory, P.O. Box 9, Observatory, Cape Town, 7935, South Africa

4 Southern African Large Telescope, P.O. Box 9, Observatory, Cape Town, 7935, South Africa

5 Departamento de Fisica, Facultad de Ciencias Naturales, Universidad de Atacama, Copayapu 485, Copiapo, Chile

1 Introduction

The high luminosity and large age of RR Lyrae type variables make them ideal distance indicators and tracers for the study of the structure and kinematics of old Galactic subsystems—the halo and the thick disk. However, the number of RR Lyrae variables in the extended solar neighborhood with both precise photometry and bona fide radial velocities is rather limited—a total of about 400 stars (Dambis et al. 2013). That is why we started a program aimed at obtaining photometric observations and radial-velocity measurements for the greatest possible number of RR Lyraes. We published the first results of our photometric observations in our previous papers (Berdnikov et al. 2011a,b, 2012, 2014), and another paper is now in preparation.

Our observations of the RR Lyrae variable SW Dor resulted in a phased light curve with a large scatter, especially near maximum brightness, which is indicative of the Blazhko effect. The aim of this study is to determine the period of the Blazhko effect and investigate the pulsation period changes in SW Dor, and to this end we compiled all the available photometric data for this star.

2 Observational data

We performed CCD observations of SW Dor during two observing seasons from December 2012 through January 2014 (JD interval JD 2456264–56671) with the 76-cm telescope of the South African Astronomical Observatory (SAAO) in South Africa using SBIG CCD ST-10XME camera equipped with BVI_c-band filters of the Kron–Cousins system (Cousins 1976). A description of the observing data reduction technique can be found in our previous paper

Published online: 29 August 2016

Table 1 CCD observations of SW Dor

HJD 2400000+	Filter	Magnitude	HJD 2400000+	Filter	Magnitude	HJD 2400000+	Filter	Magnitude
56264.3359	B	13.873	56264.3364	V	13.599	56264.3368	I_c	13.216
56265.3217	B	13.526	56265.3223	V	13.364	56265.3228	I_c	13.080
56268.3613	B	14.711	56268.3619	V	14.286	56268.3624	I_c	13.678
56269.3221	B	14.623	56269.3227	V	14.185	56269.3232	I_c	13.566
56270.3347	B	14.665	56270.3353	V	14.194	56270.3358	I_c	13.584
56273.3233	B	14.218	56273.3239	V	13.870	56273.3243	I_c	13.354
56277.3627	B	13.976	56277.3636	V	13.676	56277.3643	I_c	13.297
56278.3769	B	14.622	56278.3777	V	14.206	56278.3783	I_c	13.630
56278.4162	B	13.868	56278.4168	V	13.646	56278.4173	I_c	13.267
56278.4354	B	13.596	56278.4360	V	13.429	56278.4364	I_c	13.152
56278.4972	B	13.835	56278.4978	V	13.600	56278.4982	I_c	13.214
56279.3744	B	14.706	56279.3749	V	14.227	56279.3753	I_c	13.661
56280.4762	B	14.667	56280.4768	V	14.234	56280.4773	I_c	13.654
56280.4882	B	14.604	56280.4890	V	14.160	56280.4896	I_c	13.596
56280.4986	B	14.449	56280.4991	V	14.050	56280.4995	I_c	13.534
56280.5061	B	14.214	56280.5067	V	13.910	56280.5072	I_c	13.444
56280.5122	B	14.145	56280.5128	V	13.773	56280.5133	I_c	13.388
56281.3666	B	14.623	56281.3672	V	14.146	56281.3676	I_c	13.540
56282.3410	B	14.461	56282.3416	V	14.057	56282.3421	I_c	13.469
56283.4100	B	14.479	56283.4106	V	14.081	56283.4110	I_c	13.475
56284.4277	B	14.463	56284.4284	V	14.024	56284.4290	I_c	13.428
56286.3658	B	13.681	56286.3666	V	13.445	56286.3672	I_c	13.107
56287.3194	B	14.610	56287.3200	V	14.221	56287.3205	I_c	13.619
56288.3433	B	14.759	56288.3439	V	14.299	56288.3444	I_c	13.713
56290.3153	B	14.693	56290.3159	V	14.244	56290.3164	I_c	13.599
56291.3077	B	14.565	56291.3083	V	14.154	56291.3088	I_c	13.533
56291.3292	B	14.693	56291.3297	V	14.193	56291.3302	I_c	13.576
56292.3058	B	14.403	56292.3064	V	14.019	56292.3069	I_c	13.429
56294.2971	B	13.906	56294.2977	V	13.654	56294.2981	I_c	13.235
56294.3175	B	14.045	56294.3181	V	13.736	56294.3186	I_c	13.275
56294.3614	B	14.260	56294.3621	V	13.866	56294.3627	I_c	13.339
56295.2928	B	13.404	56295.2934	V	13.291	56295.2939	I_c	13.026
56295.3137	B	13.620	56295.3143	V	13.443	56295.3148	I_c	13.122
56296.2759	B	14.476	56296.2765	V	14.060	56296.2770	I_c	13.553
56296.2856	B	14.137	56296.2861	V	13.807	56296.2866	I_c	13.337
56296.2976	B	13.518	56296.2982	V	13.327	56296.2987	I_c	13.062
56296.3120	B	13.189	56296.3126	V	13.075	56296.3131	I_c	12.892
56296.3340	B	13.360	56296.3346	V	13.211	56296.3350	I_c	12.978

(Berdnikov et al. 2012). We acquired a total of 768 CCD frames with photometric errors close to $0.^{m}01$. We also used the Las Cumbres Observatory Global Telescope (LCOGT) Network (Brown et al. 2013) to acquire 801 CCD BVI_c frames during the time interval JD 2456635–56688. We reduce LCOGT observations by performing differential photometry relative to secondary standards whose magnitudes we determined based on observations made in SAAO; the photometric errors of these reduced observations are close to $0.^{m}02$–$0.^{m}03$.

We present all our observations in Table 1 (its complete version is available in electronic form) and show them graphically in Fig. 1.

In addition to our observations we used photographic measurements downloaded from DASCH database of digitized astronomical plate data from Harvard University

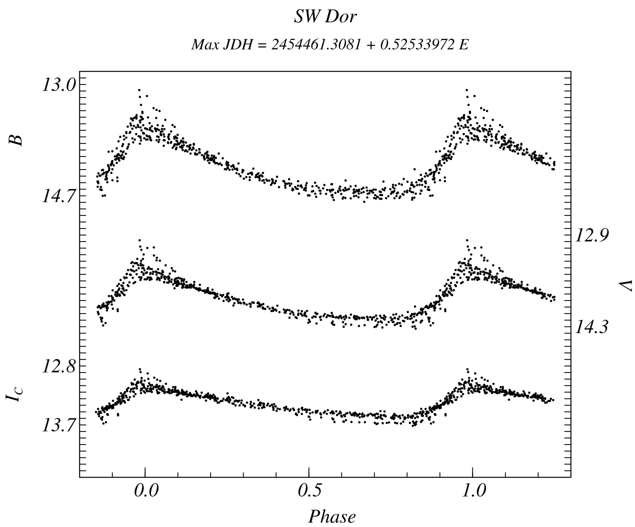

Fig. 1 BVI_c-band phased light curves of the RR Lyrae type star SW Dor. The large scatter is due to the Blazhko effect

(Grindlay et al. 2009), B- and V-band photographic observations from Butler (1978), and CCD observations from ASAS-3 (Pojmanski 2002) and OGLE-3 (Soszynski et al. 2009) and OGLE-4 (Soszynski et al. 2016) catalogs. Table 2 summarizes the information about the number of observations used.

The oldest plate in Harvard plate library bearing the image of SW Dor was acquired in 1890 and the most recent CCD frame was obtained in 2015, making up for a total time span of 125 years.

3 Pulsation period changes

We investigate the pulsation period changes in SW Dor using the standard technique of the analysis of $O-C$ diagrams. The most accurate technique for determining the $O-C$ residuals is the Hertzsprung (1919) method whose computer implementation is described by Berdnikov (1992). Table 3 lists the results of the $O-C$ calculation of seasonal light curves of SW Dor. The first and second columns give the inferred time of maximum brightness and its standard error, respectively; the third column gives the type of observations used (see Table 2); the fourth and fifth columns give the number of epoch, E, and the $O-C$ residual (in days), and the sixth and seventh columns give the number of observations, N, and the data source (see Table 2), respectively. The data from Table 3 are shown in the $O-C$ diagram (Fig. 2) by the circles (photographic observations of Butler (1978) and CCD observations) and squares (Harvard photographic observations) with vertical $O-C$ error bars which are smaller than symbols.

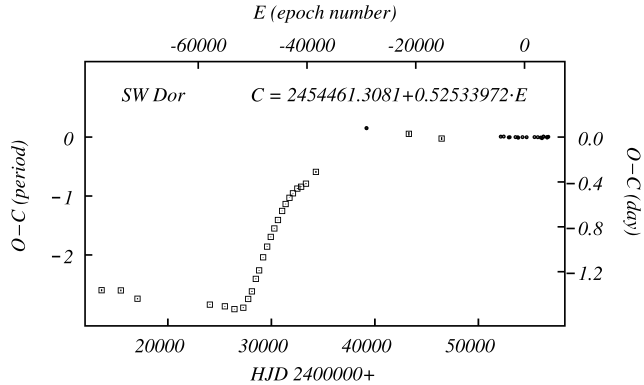

Fig. 2 $O-C$ diagram of SW Dor

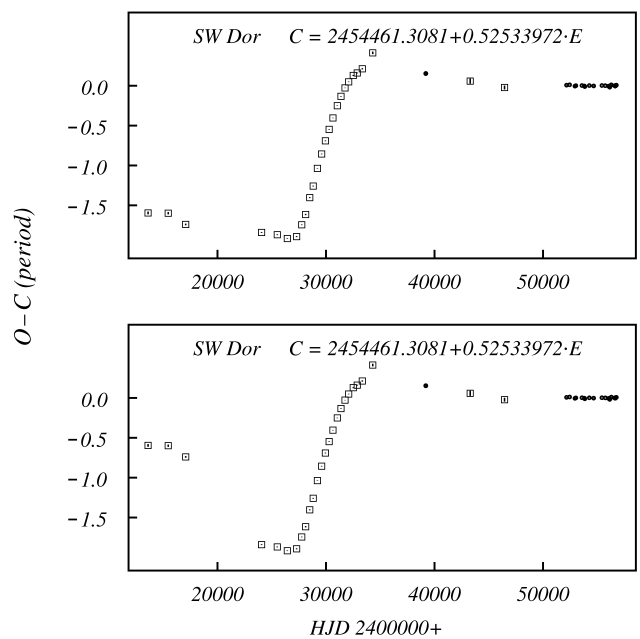

Fig. 3 Possible variants of the $O-C$ diagram of SW Dor

The $O-C$ diagram can be represented as a sequence of straight-line fragments and this behavior is indicative of at least three abrupt period changes. Table 4 lists the ephemerides for different time intervals. The last row gives the current ephemeris based on CCD observations exclusively.

Note that because of the small number of observations prior to JD 2413000 and in the JD 2435000–2450000 time interval, epoch miscalculations are possible, resulting in different variants of the $O-C$ diagram, some of which are shown in Fig. 3.

We found, based on our CCD observations, that maxima in the B-band filter occur $0^{\rm d}\!.0015$ before the corresponding maxima in the V-band filter and maxima in the V-band filter occur $0^{\rm d}\!.0015$ before the corresponding maxima in the I_c-band filter. We applied these corrections when constructing the diagrams in Figs. 2 and 3 and determin-

Table 2 Observational data for SW Dor

Data source	Number of observations	Type of observations	JD interval
DASCH (Grindlay et al. 2009)	1299	Photographic (pg)	2411621–2447511
This paper	518	CCD (B)	2456265–2456688
This paper	520	CCD (V)	2456265–2456688
This paper	531	CCD (I_c)	2456265–2456688
ASAS-3 (Pojmanski 2002)	438	CCD (V)	2451868–2455157
OGLE-3 (Soszynski et al. 2009)	38	CCD (V)	2452996–2454487
OGLE-3 (Soszynski et al. 2009)	381	CCD (I_c)	2452166–2454540
OGLE-4 (Soszynski et al. 2016)	45	CCD (V)	2455267–2456681
OGLE-4 (Soszynski et al. 2016)	402	CCD (I_c)	2455260–2457144
Butler (1978)	34	Photographic B (pgB)	2439040–2439552
Butler (1978)	28	Photographic V (pgV)	2439053–2439553

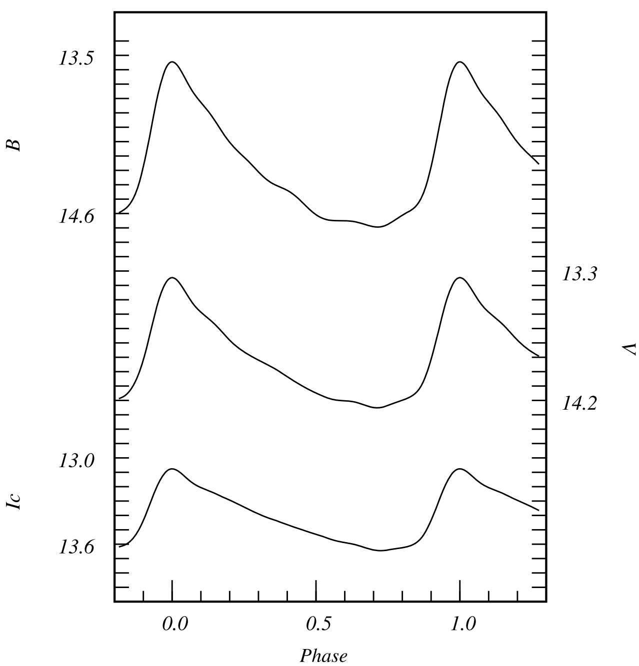

Fig. 4 B-, V- and I_c-band template curves of SW Dor

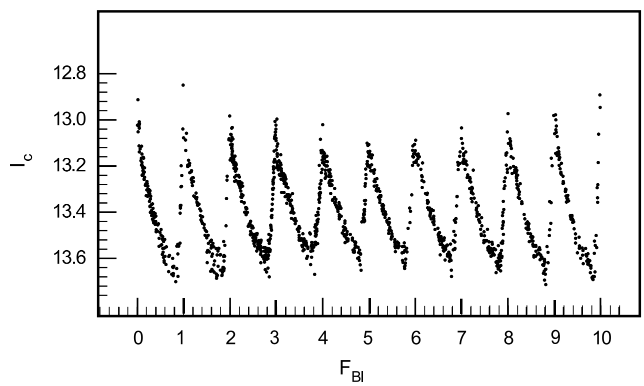

Fig. 5 Resulting combined I_c-band light curve of SW Dor for $P_{Bl} = 80\overset{d}{.}9$; F_{Bl} is the sum of the pulsation phase and the bin number for 10 bins of Blazhko period

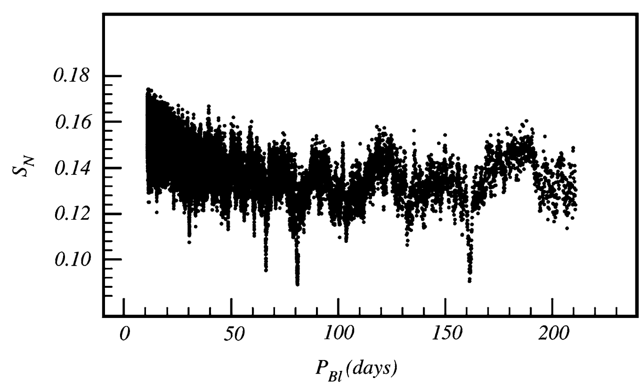

Fig. 6 Dependence of the normalized scattering parameter S_N on the trial period P_{Bl} for I_c-band observations of SW Dor

ing the ephemerides (Table 4), which therefore refer to the V-band light curve. The $O - C$ residuals shown in Figs. 2 and 3 and listed in Table 3 are computed with the current ephemeris.

Note that the results concerning period changes that we report in this paper are based on concrete light-curve templates and we therefore present these templates in Table 5 so that they can be used in future studies and for comparison with our data in the case of the use of other templates. Table 5 lists the B-, V- and I_c-band magnitudes of SW Dor at phases from 0 to 0.995 with a step of 0.005; these template curves, which are shown graphically in Fig. 4, are based on our CCD observations (Table 1).

4 The Blazhko effect

When observing the star RW Dra, S.N. Blazhko found periodic variations of the shape of its light curve (Blazhko 1907). This phenomenon has been called the Blazhko effect after its discoverer. The pulsation periods of RR Lyrae type

Table 3 Times of maximum brightness of SW Dor

Max HJD	Error (days)	Band	E	$O-C$ (days)	N	Data source
2413603.7476	0.0092	pg	−77771	−1.3651	15	DASCH
2415461.8725	0.0076	pg	−74234	−1.3668	10	DASCH
2417071.4394	0.0054	pg	−71170	−1.4408	13	DASCH
2424064.7090	0.0030	pg	−57858	−1.4936	51	DASCH
2425510.9543	0.0028	pg	−55105	−1.5085	73	DASCH
2426437.1031	0.0022	pg	−53342	−1.5337	71	DASCH
2427292.8942	0.0034	pg	−51713	−1.5209	78	DASCH
2427764.7273	0.0022	pg	−50815	−1.4429	64	DASCH
2428124.6525	0.0043	pg	−50130	−1.3754	48	DASCH
2428502.4832	0.0033	pg	−49411	−1.2640	32	DASCH
2428821.4404	0.0028	pg	−48804	−1.1880	36	DASCH
2429208.2069	0.0018	pg	−48068	−1.0716	70	DASCH
2429598.1039	0.0023	pg	−47326	−0.9766	42	DASCH
2429945.9655	0.0027	pg	−46664	−0.8899	45	DASCH
2430290.1384	0.0022	pg	−46009	−0.8145	50	DASCH
2430640.0900	0.0017	pg	−45343	−0.7391	91	DASCH
2431043.1062	0.0018	pg	−44576	−0.6586	58	DASCH
2431381.4868	0.0022	pg	−43932	−0.5967	89	DASCH
2431752.9574	0.0015	pg	−43225	−0.5413	129	DASCH
2432089.7402	0.0021	pg	−42584	−0.5012	69	DASCH
2432512.6807	0.0034	pg	−41779	−0.4592	36	DASCH
2432880.4350	0.0028	pg	−41079	−0.4427	51	DASCH
2433345.9134	0.0043	pg	−40193	−0.4153	42	DASCH
2434307.9156	0.0086	pg	−38362	−0.3102	10	DASCH
2439190.8133	0.0036	pgV	−29068	0.0802	28	Butler (1978)
2439200.7936	0.0030	pgB	−29049	0.0791	34	Butler (1978)
2443287.8865	0.0169	pg	−21166	0.0268	12	DASCH
2446452.4909	0.0129	pg	−15142	−0.0149	14	DASCH
2452164.0013	0.0031	V	−4373	0.0038	110	ASAS-3
2452449.7886	0.0016	I_c	−3829	0.0063	95	OGLE-3
2452941.4977	0.0036	V	−2893	−0.0026	110	ASAS-3
2453025.5551	0.0017	I_c	−2733	0.0004	95	OGLE-3
2453588.1948	0.0014	I_c	−1662	0.0014	96	OGLE-3
2453810.4104	0.0036	V	−1239	−0.0018	110	ASAS-3
2453852.9590	0.0027	V	−1158	−0.0057	38	OGLE-3
2454266.9334	0.0017	I_c	−370	0.0010	95	OGLE-3
2454665.6639	0.0033	V	389	−0.0013	108	ASAS-3
2455425.8333	0.0013	I_c	1836	0.0014	100	OGLE-4
2455740.5107	0.0014	I_c	2435	0.0004	100	OGLE-4
2456036.2737	0.0014	I_c	2998	−0.0029	100	OGLE-4
2456147.1137	0.0017	V	3209	−0.0096	45	OGLE-4
2456290.5440	0.0016	B	3482	0.0030	63	This paper
2456290.5449	0.0015	V	3482	0.0039	64	This paper
2456290.5461	0.0015	I_c	3482	0.0051	64	This paper
2456642.5170	0.0009	V	4152	−0.0016	193	This paper
2456643.0408	0.0008	B	4153	−0.0032	193	This paper
2456643.0437	0.0009	I_c	4153	−0.0003	191	This paper

Table 3 (*Continued*)

Max HJD	Error (days)	Band	E	$O-C$ (days)	N	Data source
2456657.2254	0.0007	B	4180	−0.0027	262	This paper
2456657.2274	0.0007	V	4180	−0.0007	263	This paper
2456658.2806	0.0008	I_c	4182	0.0018	276	This paper
2456758.6224	0.0014	I_c	4373	0.0037	102	OGLE-4

Table 4 Ephemerides of SW Dor

JD interval	T_0 (HJD)		Period (days)	
2411621–2426900	2420013.8588	±0.0095	0.52533320	±0.00000098
2426900–2432000	2429511.9077	±0.0074	0.52546035	±0.00000285
2432000–2440000	2435647.6361	±0.0042	0.52538322	±0.00000074
2452000–2457144	2454461.3081	±0.0009	0.52533972	±0.00000025

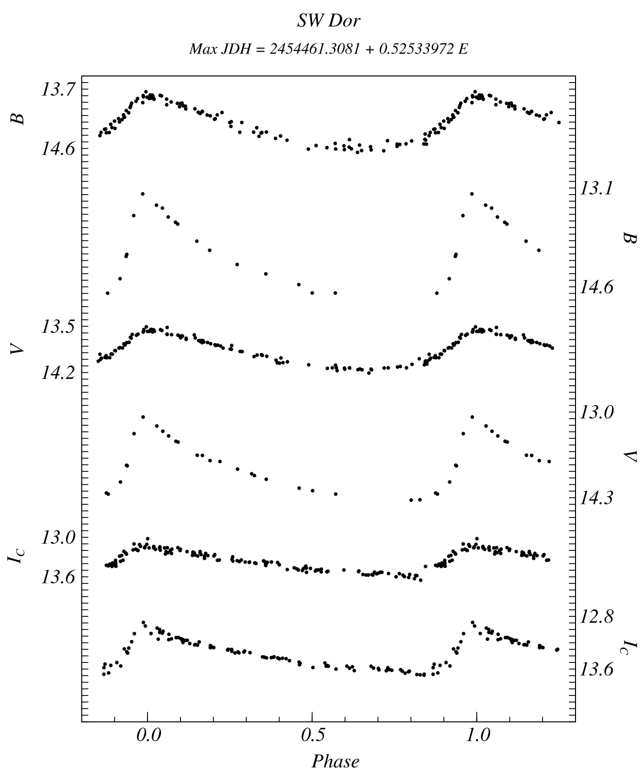

Fig. 7 B-, V- and I_c-band phased light curves of SW Dor in narrow Blazhko phase bins corresponding to the maximum and minimum amplitude

variables are close to 0.5 days, whereas the periods of the Blazhko effect are longer by a factor of 10–1000, making the search and investigation of this effect a challenging task. Because of this the Blazhko effect has been long believed to be a rare phenomenon. However, the results of recent dedicated ground-based (Drake et al. 2014; Jurcsik et al. 2009; Le Borgne et al. 2012) and spaceborne (Szabo et al. 2014; Benko et al. 2014; Benko and Szabo 2015; Molnar et al. 2015) projects showed that the fraction of fundamental-mode RR Lyraes with the Blazhko effect amounts to 50% of all stars studied (Jurcsik et al. 2009; Nemec et al. 2013; Molnar et al. 2015).

The telescopes of the above projects monitor only a small fraction of the sky and therefore the overwhelming majority of RR Lyraes have not yet been investigated for the presence of the Blazhko effect. In some cases the Blazhko effect is found accidentally as a result of unrelated projects, like in our case with SW Dor.

To determine the period of the Blazhko effect we used the method developed by Goranskii (1976), which consists in the following. For each trial period P_{Bl} of the Blazhko effect all observations are subdivided into (in our case) 10 equal phase intervals, and inside each such interval observations are sorted by the phase of the main period. The total scattering parameter S_N is computed, which is equal to the normalized sum of squared deviations of each successive point of the combined light curve from the previous point (in terms of phase). In the case of the true P_{Bl} value observations in each of the 10 intervals (Fig. 5) are practically unaffected by the scattering due to the Blazhko effect and therefore the scattering parameter S_N is minimal (Fig. 6).

Unfortunately, the low accuracy of photographic measurements and ASAS-3 CCD observations (SW Dor is close the magnitude limit for this survey and that is why its Blazhko effect was not discovered by Szczygiel and Fabrycky (2007), who analyzed all RR Lyraes found in the ASAS-3 catalog) made it impossible to determine P_{Bl}. We therefore had to restrict our analysis to our own observations (Table 1) and those acquired within the framework of OGLE-3 (Soszynski et al. 2009) and OGLE-4 (Soszynski et al. 2016) surveys and use I_c-band measurements exclusively, because OGLE data contain only 83 V-band mea-

Table 5 B-, V- and I_c-band template curves of SW Dor

Phase	B	V	I_c	Phase	B	V	I_c	Phase	B	V	I_c	Phase	B	V	I_c
0.000	13.545	13.346	13.076	0.250	14.208	13.863	13.341	0.500	14.608	14.148	13.530	0.750	14.675	14.236	13.641
0.005	13.547	13.348	13.078	0.255	14.217	13.869	13.346	0.505	14.615	14.153	13.534	0.755	14.670	14.232	13.639
0.010	13.553	13.353	13.080	0.260	14.227	13.875	13.351	0.510	14.621	14.158	13.537	0.760	14.664	14.228	13.638
0.015	13.562	13.360	13.085	0.265	14.237	13.881	13.356	0.515	14.626	14.162	13.540	0.765	14.658	14.224	13.636
0.020	13.574	13.370	13.090	0.270	14.247	13.887	13.361	0.520	14.631	14.167	13.544	0.770	14.651	14.220	13.634
0.025	13.589	13.382	13.097	0.275	14.257	13.893	13.366	0.525	14.635	14.171	13.548	0.775	14.644	14.216	13.632
0.030	13.605	13.396	13.105	0.280	14.268	13.898	13.371	0.530	14.639	14.175	13.551	0.780	14.638	14.212	13.631
0.035	13.622	13.411	13.113	0.285	14.279	13.904	13.376	0.535	14.642	14.179	13.555	0.785	14.631	14.208	13.629
0.040	13.641	13.426	13.122	0.290	14.289	13.909	13.381	0.540	14.644	14.183	13.559	0.790	14.624	14.205	13.627
0.045	13.659	13.442	13.131	0.295	14.300	13.915	13.386	0.545	14.646	14.186	13.562	0.795	14.618	14.201	13.626
0.050	13.678	13.459	13.140	0.300	14.311	13.920	13.391	0.550	14.647	14.189	13.565	0.800	14.612	14.198	13.624
0.055	13.696	13.475	13.149	0.305	14.321	13.925	13.396	0.555	14.648	14.192	13.568	0.805	14.606	14.195	13.623
0.060	13.714	13.490	13.157	0.310	14.331	13.930	13.400	0.560	14.649	14.194	13.571	0.810	14.601	14.192	13.621
0.065	13.731	13.505	13.165	0.315	14.340	13.935	13.404	0.565	14.650	14.196	13.574	0.815	14.595	14.188	13.619
0.070	13.747	13.519	13.173	0.320	14.350	13.940	13.408	0.570	14.650	14.198	13.577	0.820	14.590	14.184	13.616
0.075	13.762	13.533	13.180	0.325	14.358	13.946	13.412	0.575	14.650	14.199	13.579	0.825	14.584	14.180	13.614
0.080	13.777	13.545	13.186	0.330	14.366	13.951	13.415	0.580	14.650	14.200	13.582	0.830	14.578	14.175	13.610
0.085	13.790	13.557	13.192	0.335	14.374	13.956	13.419	0.585	14.650	14.201	13.584	0.835	14.571	14.168	13.606
0.090	13.803	13.568	13.197	0.340	14.380	13.961	13.422	0.590	14.650	14.202	13.586	0.840	14.563	14.161	13.601
0.095	13.816	13.577	13.202	0.345	14.387	13.967	13.425	0.595	14.650	14.202	13.587	0.845	14.554	14.153	13.595
0.100	13.828	13.587	13.207	0.350	14.393	13.972	13.429	0.600	14.650	14.203	13.589	0.850	14.542	14.142	13.588
0.105	13.839	13.595	13.211	0.355	14.398	13.977	13.432	0.605	14.651	14.203	13.591	0.855	14.529	14.130	13.580
0.110	13.851	13.604	13.215	0.360	14.403	13.983	13.435	0.610	14.651	14.204	13.593	0.860	14.514	14.116	13.570
0.115	13.863	13.612	13.219	0.365	14.407	13.989	13.438	0.615	14.652	14.205	13.594	0.865	14.495	14.099	13.558
0.120	13.875	13.620	13.223	0.370	14.412	13.995	13.441	0.620	14.653	14.206	13.596	0.870	14.474	14.080	13.545
0.125	13.888	13.629	13.227	0.375	14.416	14.002	13.445	0.625	14.654	14.208	13.598	0.875	14.449	14.059	13.531
0.130	13.901	13.637	13.231	0.380	14.420	14.008	13.448	0.630	14.656	14.210	13.601	0.880	14.421	14.035	13.515
0.135	13.915	13.646	13.235	0.385	14.425	14.014	13.452	0.635	14.658	14.212	13.603	0.885	14.390	14.008	13.497
0.140	13.929	13.655	13.239	0.390	14.429	14.021	13.456	0.640	14.660	14.214	13.606	0.890	14.355	13.979	13.477
0.145	13.943	13.664	13.243	0.395	14.434	14.028	13.460	0.645	14.662	14.217	13.608	0.895	14.316	13.948	13.457
0.150	13.958	13.674	13.248	0.400	14.439	14.035	13.464	0.650	14.664	14.220	13.611	0.900	14.274	13.914	13.434
0.155	13.974	13.684	13.253	0.405	14.445	14.041	13.467	0.655	14.667	14.223	13.614	0.905	14.230	13.878	13.411
0.160	13.989	13.694	13.257	0.410	14.451	14.048	13.471	0.660	14.670	14.226	13.618	0.910	14.183	13.841	13.387
0.165	14.005	13.705	13.262	0.415	14.458	14.055	13.475	0.665	14.673	14.230	13.621	0.915	14.133	13.802	13.361
0.170	14.020	13.716	13.267	0.420	14.465	14.061	13.479	0.670	14.676	14.233	13.624	0.920	14.082	13.762	13.336
0.175	14.035	13.727	13.272	0.425	14.473	14.068	13.483	0.675	14.679	14.237	13.627	0.925	14.030	13.722	13.310
0.180	14.050	13.738	13.277	0.430	14.481	14.074	13.487	0.680	14.682	14.240	13.630	0.930	13.978	13.682	13.284
0.185	14.065	13.749	13.282	0.435	14.490	14.080	13.491	0.685	14.685	14.243	13.633	0.935	13.926	13.642	13.259
0.190	14.079	13.760	13.286	0.440	14.499	14.087	13.494	0.690	14.688	14.246	13.636	0.940	13.876	13.602	13.234
0.195	14.092	13.771	13.291	0.445	14.508	14.092	13.497	0.695	14.690	14.248	13.639	0.945	13.827	13.565	13.211
0.200	14.105	13.781	13.296	0.450	14.518	14.098	13.501	0.700	14.692	14.250	13.641	0.950	13.780	13.529	13.188
0.205	14.117	13.791	13.300	0.455	14.528	14.104	13.504	0.705	14.693	14.251	13.642	0.955	13.737	13.495	13.167
0.210	14.129	13.800	13.305	0.460	14.538	14.109	13.507	0.710	14.694	14.252	13.644	0.960	13.697	13.465	13.149
0.215	14.140	13.810	13.309	0.465	14.547	14.114	13.510	0.715	14.694	14.252	13.645	0.965	13.661	13.437	13.132
0.220	14.150	13.818	13.314	0.470	14.557	14.119	13.512	0.720	14.694	14.251	13.645	0.970	13.630	13.413	13.117
0.225	14.160	13.827	13.318	0.475	14.567	14.124	13.515	0.725	14.693	14.250	13.645	0.975	13.604	13.392	13.104
0.230	14.170	13.835	13.322	0.480	14.576	14.129	13.518	0.730	14.691	14.248	13.645	0.980	13.582	13.375	13.094
0.235	14.179	13.842	13.327	0.485	14.585	14.134	13.521	0.735	14.688	14.245	13.644	0.985	13.565	13.363	13.086
0.240	14.189	13.849	13.332	0.490	14.593	14.139	13.524	0.740	14.684	14.243	13.644	0.990	13.554	13.353	13.081
0.245	14.198	13.856	13.336	0.495	14.601	14.144	13.527	0.745	14.680	14.239	13.642	0.995	13.547	13.348	13.078

Table 6 Amplitudes and phases of the pulsation and modulation frequency components of SW Dor

Name of frequency	Frequency (d^{-1})	Amplitude (mag)	Phase (rad/2π)
f_0	$1.903532 \pm 7.3 \times 10^{-7}$	0.2028 ± 0.0013	0.7940 ± 0.0011
$2f_0$	$3.807064 \pm 1.8 \times 10^{-6}$	0.0838 ± 0.0013	0.0213 ± 0.0025
$3f_0$	$5.710595 \pm 2.9 \times 10^{-6}$	0.0510 ± 0.0013	0.2602 ± 0.0041
$4f_0$	$7.614117 \pm 5.0 \times 10^{-6}$	0.0297 ± 0.0013	0.0638 ± 0.0072
$5f_0$	$9.517639 \pm 9.2 \times 10^{-6}$	0.0161 ± 0.0013	0.8254 ± 0.0132
Triplet components			
$f_0 - f_b$	$1.891166 \pm 9.3 \times 10^{-6}$	0.0161 ± 0.0013	0.8600 ± 0.0133
$f_0 + f_b$	$1.915927 \pm 9.9 \times 10^{-6}$	0.0155 ± 0.0013	0.9336 ± 0.0142
$2f_0 - f_b$	$3.794708 \pm 1.2 \times 10^{-5}$	0.0126 ± 0.0013	0.4896 ± 0.0171
$2f_0 + f_b$	$3.819469 \pm 1.2 \times 10^{-5}$	0.0130 ± 0.0013	0.5876 ± 0.0172
$3f_0 - f_b$	$5.698219 \pm 1.2 \times 10^{-5}$	0.0120 ± 0.0013	0.8297 ± 0.0181
$4f_0 - f_b$	$7.601761 \pm 1.3 \times 10^{-5}$	0.0117 ± 0.0013	0.5211 ± 0.0191
Blazhko frequency			
f_b	$0.01234 \pm 1.5 \times 10^{-5}$	0.0102 ± 0.0013	0.5844 ± 0.0211

surements compared to 783 observations in I_c. The scattering parameter for 1314 I_c-band observations (Fig. 6) reaches its minimum value at P_{Bl} close to $80\overset{\mathrm{d}}{.}88$.

We also calculated the frequency spectra using the PERIOD04 program (Lenz and Breger 2005). The most prominent frequencies are listed in Table 6. We found the Blazhko frequency to be 0.01234 d^{-1} corresponding to the Blazhko period of $81\overset{\mathrm{d}}{.}04$. The six triplet components yield a mean Blazhko frequency of 0.01237 d^{-1} corresponding to the period of $80\overset{\mathrm{d}}{.}84$.

We therefore adopt the mean Blazhko period estimate of $80\overset{\mathrm{d}}{.}9$ based on both methods.

Figure 7 shows the B-, V- and I_c-band light curves of SW Dor (based on Table 1 and OGLE survey data) folded with the pulsation period for observations in the narrow bins of P_{Bl} phases corresponding to the maximum and minimum amplitude.

5 Conclusions

1. We acquired 1569 CCD frames in the BVI_c filters for the RR Lyrae type variable SW Dor. Our observations resulted in a phased light curve with a large scatter, especially near maximum brightness, which allowed us to reveal the Blazhko effect.
2. Our observations combined with OGLE data allowed us to determine the period of the Blazhko effect $P_{Bl} \sim 80\overset{\mathrm{d}}{.}9$.
3. We constructed the $O - C$ diagram for SW Dor, which, because of incorporating photographic observations based on Harvard plate measurements, spans a 125-year long time interval, allowed us to reveal at least three sudden changes of the pulsation period.

Acknowledgements We thank the anonymous reviewer for the helpful and valuable comments, which improved the final version of the paper. This study was supported by the Russian Foundation for Basic Research (grant no. 14-02-00472) and the National Research Foundation of South Africa. This work makes use of observations from the LCOGT network, from the South African Astronomical Observatory (SAAO), and data from the DASCH project at Harvard which is grateful for partial support from NSF grants AST-0407380, AST-0909073, and AST-1313370. The light-curve analysis was supported by the Russian Science Foundation (project no. 14-22-00041).

References

Benko, J.M., Szabo, R.: Astrophys. J. Lett. **809**, 19 (2015)
Benko, J.M., Plachy, E., Szabo, R., et al.: Astrophys. J. Suppl. Ser. **213**, 31 (2014)
Berdnikov, L.N.: Sov. Astron. Lett. **18**, 207 (1992)
Berdnikov, L.N., Kniazev, A.Yu., Sefako, R., et al.: Observatory **131**, 315 (2011a)
Berdnikov, L.N., Kniazev, A.Yu., Sefako, R., et al.: Observatory **131**, 386 (2011b)
Berdnikov, L.N., Vozyakova, O.V., Kniazev, A.Yu., et al.: Astron. Rep. **56**, 290 (2012)
Berdnikov, L.N., Dambis, A.K., Kniazev, A.Yu., et al.: Observatory **134**, 206 (2014)
Blazhko, S.: Astron. Nachr. **175**, 325 (1907)
Brown, T.M., Baliber, N., Bianco, F.B., et al.: Publ. Astron. Soc. Pac. **125**, 1031 (2013)
Butler, C.J.: Astron. Astrophys. Suppl. Ser. **32**, 83 (1978)
Cousins, A.W.J.: Mem. R. Astron. Soc. **81**, 25 (1976)
Dambis, A.K., Berdnikov, L.N., Kniazev, A.Yu., et al.: Mon. Not. R. Astron. Soc. **435**, 3206 (2013)
Drake, A.J., Graham, M.J., Djorgovski, S.G., et al.: Astrophys. J. Suppl. Ser. **213**, 9 (2014)
Goranskii, V.P.: Perem. Zvezdy Prilož. **2**, 323 (1976)
Grindlay, J., Tang, S., Simcoe, R., et al.: In: Preserving Astronomy's Photographic Legacy. ASP Conf. Ser., vol. 410, p. 101 (2009)

Hertzsprung, E.: Astron. Nachr. **210**, 17 (1919)
Jurcsik, J., Sodor, A., Szeidl, B., et al.: Mon. Not. R. Astron. Soc. **400**, 1006 (2009)
Le Borgne, J.-F., Klotz, A., Poretti, E., et al.: Astron. J. **144**, 39 (2012)
Lenz, P., Breger, M.: Commun. Asteroseismol. **146**, 53 (2005)
Molnar, L., Szabo, R., Moskalik, P.A., et al.: Mon. Not. R. Astron. Soc. **452**, 4283 (2015)
Nemec, J.M., Cohen, J.G., Ripepi, V., et al.: Astrophys. J. **773**, 181 (2013)
Pojmanski, G.: Acta Astron. **52**, 397 (2002)
Soszynski, I., Udalski, A., Szymanski, M.K., et al.: Acta Astron. **59**, 1 (2009)
Soszynski, I., Udalski, A., Szymanski, M.K., et al.: Acta Astron. **66**, 1 (2016)
Szabo, R., Benko, J.M., Paparò, M., et al.: Astron. Astrophys. **570**, A100 (2014)
Szczygiel, D.M., Fabrycky, D.C.: Mon. Not. R. Astron. Soc. **377**, 1263 (2007)